

Multiple ionization of C_{60} by fast Si^{q+} ions

T. Mizuno,¹ H. Tsuchida,¹ T. Majima,^{1,2} Y. Nakai,³ and A. Itoh^{1,*}

¹*Department of Nuclear Engineering, Kyoto University, Kyoto 606-8501, Japan*

²*Department of Physics, Tokyo Metropolitan University, Hachioji, Tokyo 192-0397, Japan*

³*RIKEN Nishina Center, Wako, Saitama 351-0198, Japan*

(Received 25 June 2008; revised manuscript received 26 July 2008; published 18 November 2008)

Multiple ionization of C_{60} by Si^{q+} ions ($q=1-3$) has been studied at incident energies of 0.5, 0.8, 2.0, and 6.0 MeV covering a velocity range of $v=0.85-2.93$ in atomic units. Fragment ions and secondary electrons were measured in coincidence with charge-selected outgoing projectile ions, enabling us to determine the charge state of prefragmented parent ions C_{60}^{r+} . Charge state (r) distributions correlated with the smallest fragment ions of C_m^+ ($m \leq 3$) were found to vary rather strongly depending on v and q , whereas the r distributions were less sensitive for medium sized ions of $m \geq 4$. These results reflect fairly well the difference of the amount of inelastic energy deposition estimated from the local density approximation. Experimental r distributions correlated with specific fragment ions C_m^+ ($m \leq 5$) were reproduced almost perfectly by our statistical energy deposition model. From our model calculations we also obtained the most probable values of the ionization energy associated with the production of individual fragment ions.

DOI: [10.1103/PhysRevA.78.053202](https://doi.org/10.1103/PhysRevA.78.053202)

PACS number(s): 36.40.Qv

I. INTRODUCTION

Collision-induced fragmentation of C_{60} has been extensively investigated in the past decade [1–11]. Among many valuable findings reported in these studies, one of the striking phenomena observed in fast ion collision experiments is that a C_{60} molecule is broken into small fragments even when the charge state of prefragmented ion C_{60}^{r+} is extremely low ($r \sim 3$) [8–10]. This fact implies evidently that the internal excitation plays a substantial role in C_{60} multifragmentation. Actually, in fast ion- C_{60} collisions a large amount of electronic energy deposition is predicted, from the local density approximation (LDA) [12], to reach a few keV which is comparable to an energy loss in a thin carbon foil. On the other hand, the Coulomb explosion due to the instability arising from high charge states produced in collisions plays also an important role in multifragmentation [2].

To date, the mechanism of collision-induced C_{60} fragmentation has not yet been fully understood. This is because a conventional time-of-flight measurement does not provide information about the degree of ionization r of a prefragmented ion C_{60}^{r+} , since the number of electrons emitted simultaneously are not determined in such a simple way. In order to understand the fragmentation mechanism more clearly, we developed a triple coincidence technique allowing us to make simultaneous measurement of fragment ions, outgoing projectile particles, and secondary electrons [8–11]. This technique enables us to determine total and partial r distributions of C_{60}^{r+} . Here, the term partial means a r distribution correlated with a specific fragment ion C_m^+ of fixed size m . Inversely, one can also know a fragment mass distribution correlated with a fixed charge state r of prefragmented ions. Experimental results obtained in this way have been successfully examined by the energy partition model based on the idea that the electronic energy deposition E_d is shared

between ionization and excitation with a certain partition rate [8–11]. Note, however, that the model can predict only average values of r and not reproduce the r distribution itself. It needs a more statistical approach to account for the experimental r distributions.

In our previous papers [8,9] the r distribution was investigated in detail using 2 MeV Si^{2+} ions ($v=1.69$ a.u.) undergoing single and double electron loss and capture collisions. In this work, investigation of Si^{q+} -induced multiple ionization is extended to a wider velocity range from $v=0.85$ to 2.93 a.u. and charge states $q=1-3$. As the amount of E_d is known to vary strongly with respect to both v and q in this velocity range, we achieved more detailed investigation of the relationship between E_d and the resulting r distribution correlated with size-fixed fragment ions C_m^+ of $m < 10$. It is noted that these small-size fragment ions are produced only in close encounters between collision partners. In such collisions the correlated r distribution is supposed not to depend greatly on the type of charge-charging collisions as demonstrated in [8,9] as for single electron loss and capture collisions. Hence, we limited measurements in this work to the single electron loss process. Estimation of E_d was made by using the LDA model. Present results of r distributions correlated with size-fixed fragment ions are compared with our newly developed model calculations achieved by taking account of the statistical nature of electronic energy deposition process.

II. EXPERIMENT

The experiment was performed at the QSEC 1.7-MV tandem Cockcroft-Walton accelerator facility of Kyoto University. As the experimental method and apparatus are described in [8,9], only the essential outline is given here. Projectile ions investigated are 6.0 MeV Si^{3+} , 2.0 MeV Si^{2+} , and Si^+ with energies of 0.5, 0.8, and 2.0 MeV. The incident beam was carefully collimated to smaller than 0.1 mm in diameter and was charge-purified with a magnetic charge-selector be-

*itoh@nucleng.kyoto-u.ac.jp

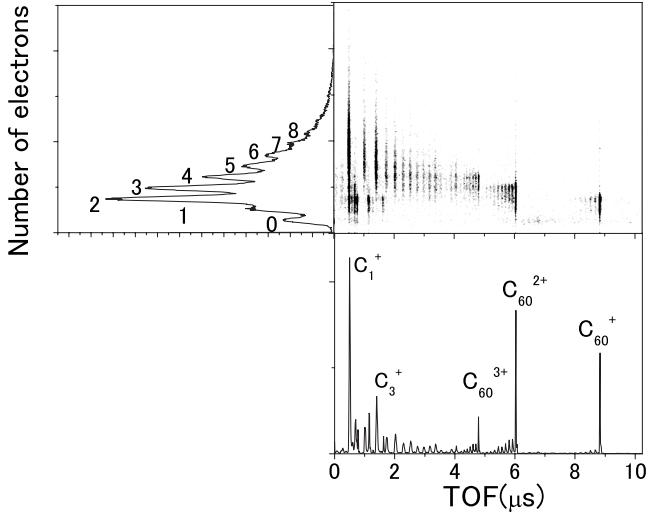
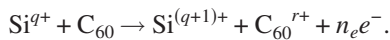


FIG. 1. 2D spectrum of time-of-flight of fragment ions and the number of secondary electrons n_e obtained for single electron loss collisions of 0.5 MeV Si^+ projectiles.

fore entering a collision chamber. A gas phase C_{60} target was produced by sublimation of high-purity (99.98%) powder at 550 °C in a temperature controlled quartz crucible. The effusive C_{60} beam was collimated to smaller than 4 mm in diameter by two apertures with diameters of 1.0 mm and 2.0 mm above the crucible. A base pressure of the target chamber was kept below 5×10^{-6} Pa. After collisions with the C_{60} target, outgoing projectiles were charge separated by an electrostatic deflector and detected by a movable semiconductor detector (SSD). Positive fragment ions and secondary electrons were extracted into opposite directions by an electric field of 615 V/cm applied perpendicular to the incident beam axis. Fragment ions were detected by a two-stage multichannel plate with a front voltage of -4.6 kV. This voltage is sufficient to detect all the fragment ions C_m^+ of $m \leq 10$ with highest detection efficiency of about 1 [7]. The mass distribution of product ions was measured by a time-of-flight (TOF) method. Secondary electrons were detected by a PIPS-type SSD detector biased at +30 kV, enabling us to obtain the number of secondary electrons n_e emitted simultaneously in a single collision. Detection of fragment ions and secondary electrons was made in coincidence with scattered ions of charge states $(q+1)$ produced in single electron loss collisions described as



Here, C_{60}^{r+} stands for a prefragmented parent ion and $n_e = r + 1$ is the number of free electrons. As mentioned in Sec. I, r distributions correlated with specific fragment ions are known to be almost the same for single electron loss and capture collisions [8,9], so that we investigate here only the single electron loss process.

An example of a two-dimensional (2D) map of TOF- n_e coincidence spectra obtained for 0.5 MeV Si^+ ions is shown in Fig. 1. Horizontal and vertical axes are the time-of-flight (μs) of fragment ions and the pulse height of electrons detected by the SSD, corresponding to the number of electrons

(n_e) as indicated in the figure. As we know both q and n_e , the charge state r of a prefragmented ion can be determined within an accuracy of better than 94% [8]. From these 2D maps one can derive the r distribution correlated with a specific fragment ion C_m^+ of any desired value of m . Also one can derive the fragment ion distribution correlated with a specific value of r . It should be pointed out that, similar to other projectile ions investigated previously [8–10], C_{60} multifragmentation is found to occur even at low charge states of, e.g., $r=3$.

III. RESULTS AND DISCUSSION

A. r distributions correlated with size-fixed fragment ions

Before a quantitative discussion of our experimental results, it might be helpful to overview the scenario of our energy partition model described previously [6,8–11]. In this model, the electronic energy deposition E_d into a target particle from an incident particle is divided between ionization (E_{ion}) and internal excitation (E_{int}) with a certain partition rate α , i.e., $E_d = E_{\text{ion}} + E_{\text{int}}$ and $E_{\text{ion}} = \alpha E_d$. The ionization energy E_{ion} is then shared between kinetic energies of all ionized electrons (E_k) and the sum of their ionization potentials (E_p) with another partition rate β as $E_{\text{ion}} = E_p + E_k$ and $E_p = \beta E_{\text{ion}} = \alpha \beta E_d$. We set $P_p = \alpha \beta$ in the following discussion. If we know the amount of E_d and the partition rates, we can deduce E_{int} and average values of r [8–11].

Figure 2 shows r distributions correlated with smaller fragment ions of C_1^+ , C_3^+ , and C_5^+ measured for various incident energies. One can see that the r distribution correlated with C_1^+ changes greatly depending on the projectile velocity v and charge state q , while such a variation becomes smaller with increasing fragment size m . As the first step to interpret these experimental r distributions, we calculated impact parameter dependent E_d by using the local density approximation (LDA) [12]. The calculation procedure is described in [11,13–15]. Briefly, the electronic energy deposition $E_d(b)$ at an impact parameter b , measured from the C_{60} center, is given by

$$E_d(b) = \frac{4\pi q_e^2}{v^2} \int_{-\infty}^{\infty} \rho(r) L(\rho(r), v) dz, \quad (1)$$

with $L(\rho, v)$ the stopping number and $\rho(r)$ the electron density of C_{60} [16]. The effective charge q_e of projectile ions used in Eq. (1) was calculated from [17]. At incident energies below 2.0 MeV ($v=1.7$ a.u.) the calculated values of q_e for Si^+ and Si^{2+} ions are 2.49 and 3.22, respectively. Note that q_e is constant for incident velocities $v \leq 1.8$ a.u. As for $v > 1.8$ a.u., q_e is velocity dependent and is calculated to be 5.04 for 6.0 MeV Si^{3+} ions ($v=2.9$ a.u.). Calculated results of $E_d(b)$ are depicted in Fig. 3 as a function of b . These values are largely different at $b < 9$ for different projectile ions. Hence, it is plausible to state that the smallest fragment ions, showing large variation of r distribution, are produced in C_{60} cage penetration collisions, while medium sized fragments are in peripheral collisions. This conclusion agrees well with our previous work concerning the scattering angle-dependent fragmentation of C_{60} [11]. The average value of E_d is estimated from

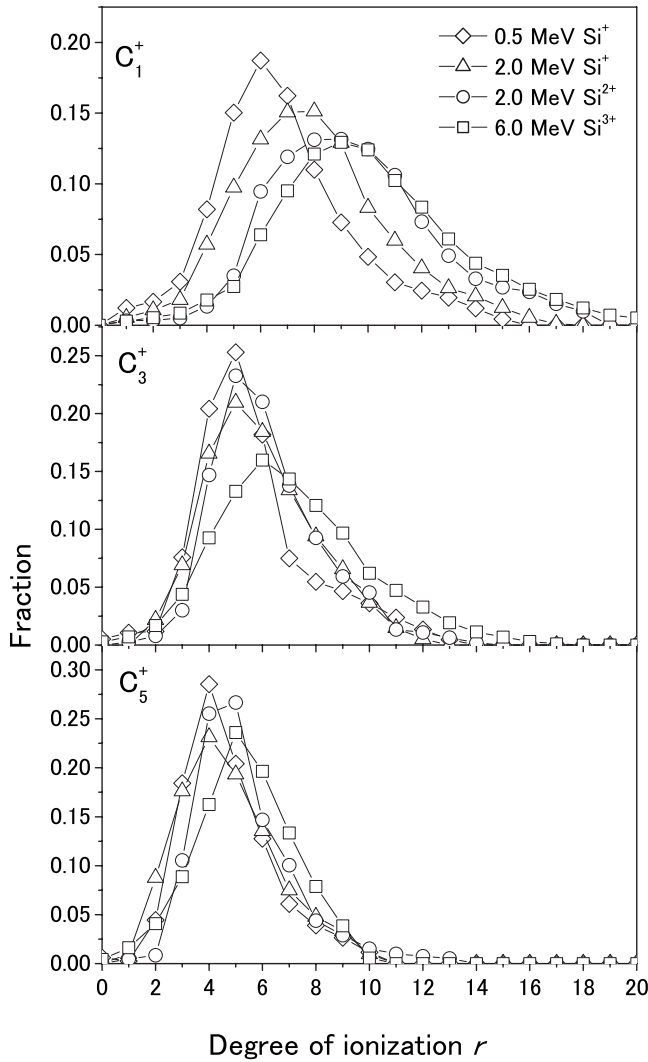


FIG. 2. r distributions of prefragmented C₆₀^{r+} ions correlated with the production of C_m⁺ ions obtained for single electron loss collisions.

$$E_d = (2\pi/\pi b_o^2) \int_0^{b_o} b E_d(b) db, \quad (2)$$

where we took $b_o=9$ a.u. as the effective molecular radius of C₆₀. The average values of E_d in eV are 550 (0.5 MeV Si⁺), 680 (0.8 MeV Si⁺), 880 (2.0 MeV Si⁺), 1470 (2.0 MeV Si²⁺), and 2560 (6.0 MeV Si³⁺).

Figure 4 shows the average value of total ionization potentials \bar{E}_p associated with the production of C₁⁺ as a function of E_d . Here, \bar{E}_p is calculated from an experimental r distribution as

$$\bar{E}_p = \sum_r F_r \left(\sum_{i=1}^r I_i \right), \quad (3)$$

where I_i is the i th ionization potential ($I_i=3.77+3.82i$) [18], and F_r is the normalized intensity of C₆₀^{r+} in experimental r distributions (see Fig. 2) with $\sum_r F_r=1$. It is noted here that more recent data of the ionization potentials available in lit-

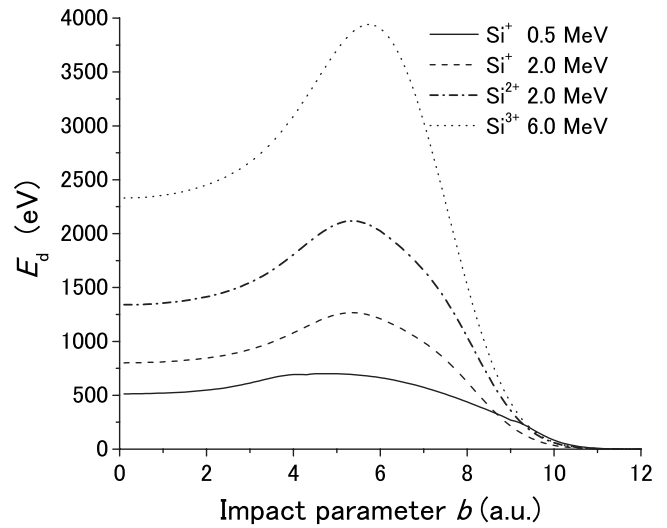


FIG. 3. Electronic energy deposition E_d calculated from LDA plotted as a function of the impact parameter b .

erature [19] are expressed as $I_i=3.85+3.25i$, giving rise to slightly lower values than the above formula. Deviation of \bar{E}_p calculated from these two formulas was 12% at most (6 MeV Si³⁺).

It is interesting to note that \bar{E}_p increases with increasing E_d but is not proportional to E_d , indicating that the degree of multiple ionization does not increase simply even if the energy deposition is large. The similar trend is also observed in H⁺-C₆₀ collisions [3]. They report that both ionization and C₂ evaporation from C₆₀ exhibit strongly a so-called velocity effect as a function of E_d . They showed that the evaporation fractions, for instance, are largely different at different velocities even if the values of E_d are the same. Qualitatively, it can certainly be stated that the degree of multiple ionization of C₆₀ may be different at different impact velocities even if E_d 's are the same. Actually, we found in our previous work that, in the same E_d but different v collisions (2 MeV Li⁺ and 0.4 MeV O⁺), multiple ionization was entirely different [10].

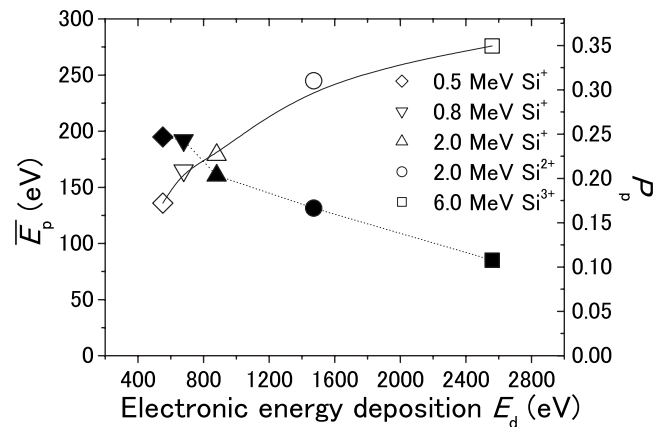


FIG. 4. Average ionization potential \bar{E}_p associated with C₁⁺ (open symbols) and the partition rate P_p (full symbols) as a function of E_d obtained for various impact energies.

B. Estimation of the partition rate P_p

The relationship between E_d and $\overline{E_p}$ shown in Fig. 4 gives quantitative information about the partition rate defined by $P_p = \alpha\beta = \overline{E_p}/E_d$. Estimated values of P_p , also shown in Fig. 4, are 0.25 (0.5 MeV Si⁺), 0.24 (0.8 MeV Si⁺), 0.20 (2.0 MeV Si⁺), 0.17 (2.0 MeV Si²⁺) and 0.11 (6.0 MeV Si³⁺). Theoretical calculations of partition rates have been performed so far for a few collision systems; 0.2–10⁴ keV H+H₂O [20] and 1.4 MeV/amu U³²⁺+Ne[21]. From [20] one can derive the partition rate α in the present velocity range as $\alpha=0.7(v=0.8)-0.85(v=3.0)$. As for β , Olson *et al.* reported $\beta=0.25$. Although these collision systems are different from each other, the magnitude of P_p as a theoretical value can be obtained to be about 0.2 in the present velocity range. It is worthwhile to point out that this theoretical value compares fairly well with our experimental results given above. Actually, in our previous works we used these two theoretical partition rates and most experimental results were successfully analyzed [8–11].

C. Calculation of r distributions with statistical energy deposition model

In this section we focus on the r distribution in more detail. As shown in Fig. 2, r distributions correlated with individual fragment ions are different widely from each other. In order to achieve more accurate statistical analysis of these r distributions, we extended a statistical energy deposition (SED) model developed on the basis of the following idea [13,14,22,23]. Since the collision time of swift ions is

considerably shorter than the typical time ($\sim 10^{-9}$ s) of any rovibrational motion of C₆₀, a swift ion is assumed to deposit a certain amount of E_d into a C₆₀ fixed in space. Outer-shell electrons are then ionized slowly (autoionization) in comparison with the collision time, and E_d may be statistically distributed among the electronic freedoms of C₆₀. Assuming the multiple ionization probability to be proportional to the volume of phase space available in the ionization state of interest, Russek and Meli [22] formulated the r -fold ionization probability P_r as

$$P_r(E_k) = C \binom{N_e}{n} g^n S_r(E_k(r)/I_1), \quad (4)$$

with

$$S_r(x) = \frac{2^{[(r-1)/2]} \pi^{(r/2)} x^{(3r-2)/2}}{(3r-2)!!}, \quad (5)$$

where N_e is the number of electrons of the target particle (we set $N_e=240$ for C₆₀), and S_r is the density of final states. The parameter g is proportional to the mean-square matrix element of single ionization. As the value of g is difficult to be estimated theoretically, we chose $g=0.007$ since this value was found to reproduce fairly well the experimental results [5]. The kinetic energy E_k carried away by the ionized r electrons is given by

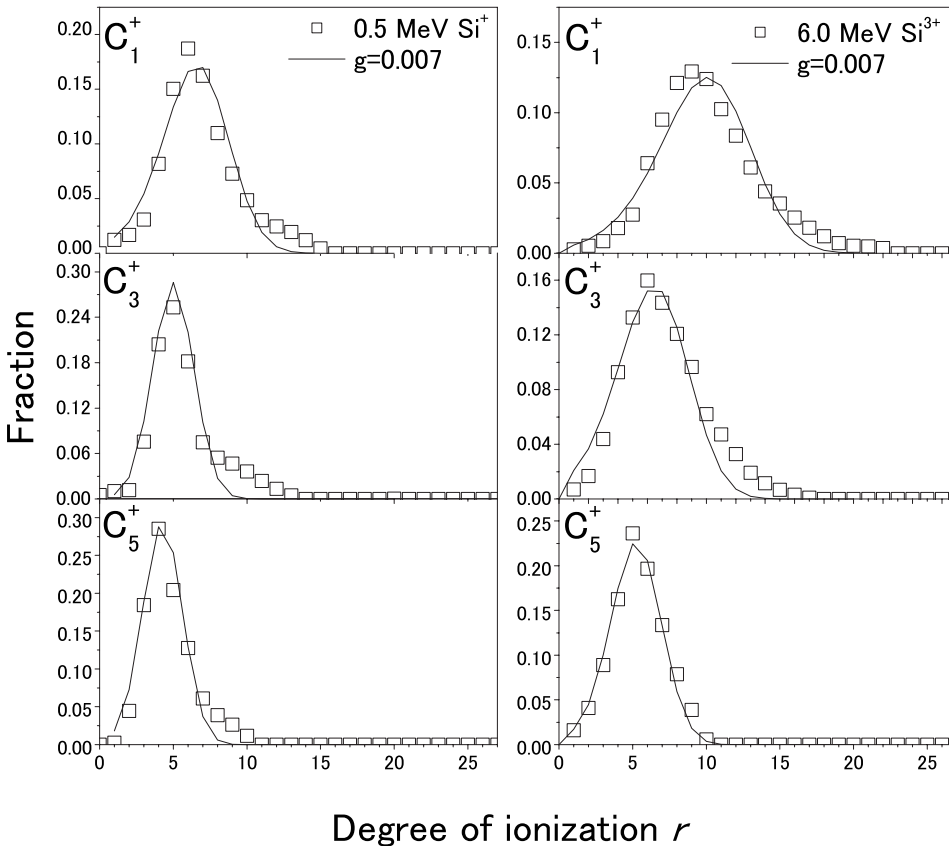


FIG. 5. SED model calculations of r distributions correlated with C⁺, C₃⁺, and C₅⁺ obtained for 0.5 MeV Si⁺ and 6.0 MeV Si³⁺ single electron loss collisions

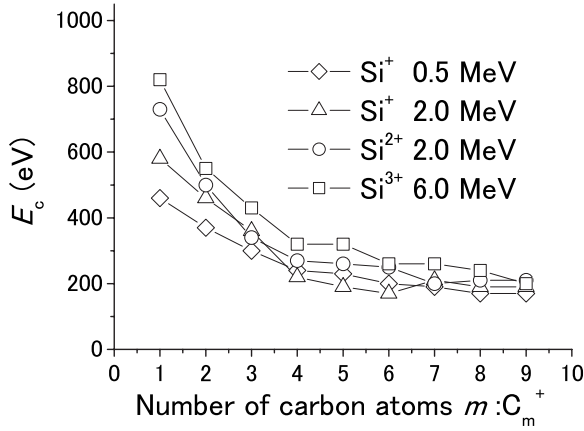


FIG. 6. The most probable ionization energies E_c derived from fitting calculations for individual fragment ions C_m^+ .

$$E_k(r) = E_{\text{ion}} - E_p = E_{\text{ion}} - \sum_{i=1}^r I_i. \quad (6)$$

We extended this SED model as follows. As the number of electronic freedoms of C₆₀ is large and the energy deposition process is essentially statistical, the internal excitation energy may be treated as a certain distribution function for which we used a Gaussian distribution as

$$w(E_{\text{ion}}) = \frac{1}{\sqrt{2\pi}\sigma} \exp\left(-\frac{(E_{\text{ion}} - E_c)^2}{2\sigma^2}\right), \quad (7)$$

where E_c is the most probable value and σ is the standard deviation. With this $w(E_{\text{ion}})$ the probability of r -fold multiple ionization can be obtained by

$$P_r = \int P_r(E_k) w(E_{\text{ion}}) dE_{\text{ion}}. \quad (8)$$

We applied this formula to our experimental r distributions by treating σ and E_c as fitting parameters. Fitting results are depicted in Fig. 5 for 0.5 MeV Si⁺ and 6 MeV Si³⁺, showing excellently good reproduction of the experimental r distributions. As the choice of g is somewhat arbitrary, we examined other values of g and obtained again good reproduction of the experimental results. It indicates that g does not affect greatly the fitting calculation. Furthermore, we also obtained from our fitting calculations the most probable ionization energies E_c for individual fragment ions. The results are presented in Fig. 6, showing several hundreds of eV for C⁺ and nearly constant values of about 250 eV for medium sized ions. It is noteworthy that the estimation of E_c is possible in our model calculations without knowledge of the kinetic energies carried away by the secondary electrons.

As shown above the SED model appears to work fairly well to account for inelastic processes of complicated collisions involving polyatomic molecules. It should, however, be pointed out that this model does not consider the electron capture which is the most dominant process in slow velocity or highly charged ion collisions. As the electron capture is a prompt process occurring within a collision time, the delayed ionization process may be affected by the charge state of the parent ion. In the present experiment, however, the incident projectile charge states are low so that the electron capture does not affect appreciably.

IV. SUMMARY

Multiple ionization of C₆₀ was investigated for Si^{q+} ($q=1-3$) ions in an energy range from 0.5 to 6.0 MeV. By means of our triple coincidence technique, precise measurements were made for the charge distribution of prefragmented C₆₀^{r+} ions in correlation with size-fixed fragment ions C_m⁺ produced in the successive C₆₀^{r+} fragmentation process. The characteristics of r distribution, exhibiting a rather strong dependence on v and q of projectile ions, were examined by energy deposition consideration with the local density approximation (LDA) [12]. The energy deposition as a function of the impact parameter reflect fairly well the tendency of our experimental r distributions. Namely, we confirmed qualitatively that the smallest fragment ions of size $m \leq 3$ are produced in collisions of impact parameters $b < 9$ and medium size ions are produced in peripheral collisions. This conclusion agrees with our previous work of scattering angle-dependent C₆₀ fragmentation [11].

From r distributions of prefragmented C₆₀^{r+} ions, we derived for the first time the partition rate P_p associated with the ionization of C₆₀. We found that the present values are quantitatively consistent with theoretical values reported for other collision systems [20,21]. The r distribution was examined in detail by our statistical energy deposition model by taking account of the statistical characteristic of internal excitation. The r distributions correlated with sized fixed specific fragment ions were reproduced fairly well by this model calculation. Moreover, we obtained the most probable ionization energies for individual fragment ions from our SED model calculations. It should be pointed out that the somewhat arbitrary parameter g contained in the SED model is rather insensitive in the fitting calculations. In conclusion, we stress that our newly developed SED model works powerfully for the analysis of multiple ionization of polyatomic molecules like C₆₀.

ACKNOWLEDGMENTS

This work was supported by a Grant-in-Aid for Scientific Research (B), Grant No. 16360474, from the Japan Society for the Promotion of Science.

- [1] E. E. B. Campbell and E. Rohmund, Rep. Prog. Phys. **63**, 1061 (2000).
- [2] S. Martin, L. Chen, A. Denis, R. Bredy, J. Bernard, and J. Désesquelles, Phys. Rev. A **62**, 022707 (2000).
- [3] J. Opitz *et al.*, Phys. Rev. A **62**, 022705 (2000).
- [4] O. Hadjar, P. Földi, R. Hoekstra, R. Morgenstern, and T. Schlathöller, Phys. Rev. Lett. **84**, 4076 (2000).
- [5] A. Reinköster, U. Werner, N. M. Kabachnik, and H. O. Lutz, Phys. Rev. A **64**, 023201 (2001).
- [6] H. Tsuchida, A. Itoh, Y. Nakai, K. Miyabe, and N. Imanishi, J. Phys. B **32**, 5289 (1999).
- [7] A. Itoh, H. Tsuchida, T. Majima, and N. Imanishi, Phys. Rev. A **59**, 4428 (1999).
- [8] T. Majima, Y. Nakai, H. Tsuchida, and A. Itoh, Phys. Rev. A **69**, 031202(R) (2004).
- [9] T. Majima, Y. Nakai, T. Mizuno, H. Tsuchida, and A. Itoh, Phys. Rev. A **74**, 033201 (2006).
- [10] T. Mizuno, T. Majima, Y. Nakai, H. Tsuchida, and A. Itoh, Nucl. Instrum. Methods Phys. Res. B **256**, 101 (2007).
- [11] T. Mizuno, D. Okamoto, T. Majima, Y. Nakai, H. Tsuchida, and A. Itoh, Phys. Rev. A **75**, 063203 (2007).
- [12] J. Lindhard and M. Scharff, Mat. Fys. Medd. K. Dan. Vidensk. Selsk. **27**, 15 (1953).
- [13] N. M. Kabachnik, V. N. Kondratyev, Z. Roller-Lutz, and H. O. Lutz, Phys. Rev. A **56**, 2848 (1997).
- [14] N. M. Kabachnik, V. N. Kondratyev, Z. Roller-Lutz, and H. O. Lutz, Phys. Rev. A **57**, 990 (1998).
- [15] P. Moretto-Capelle, D. Bordenave-Montesquieu, A. Rentenier, and A. Bordenave-Montesquieu, J. Phys. B **34**, L611 (2001).
- [16] M. J. Puska and R. M. Nieminen, Phys. Rev. A **47**, 1181 (1993).
- [17] W. Brandt and M. Kitagawa, Phys. Rev. B **25**, 5631 (1982).
- [18] H. Steger, J. Holzapfel, A. Hielscher, W. Kamke, and I. V. Hertel, Chem. Phys. Lett. **234**, 455 (1995).
- [19] H. Zettergren, H. T. Schmidt, P. Reinhard, H. Cederquist, J. Jensen, P. Hvelplund, S. Tomita, B. Manil, J. Rangama, and B. A. Huber, Phys. Rev. A **75**, 051201(R) (2007).
- [20] J. H. Miller and A. E. S. Green, Radiat. Res. **54**, 343 (1973).
- [21] R. E. Olson, J. Ullrich, and H. Schmidt-Bocking, Phys. Rev. A **39**, 5572 (1989).
- [22] A. Russek and J. Meli, Physica (Amsterdam) **46**, 222 (1970).
- [23] B. Siegmann, U. Werner, Z. Kaliman, Z. Roller-Lutz, N. M. Kabachnik, and H. O. Lutz, Phys. Rev. A **66**, 052701 (2002).